UPPSALA
UNIVERSITET

Digital Comprehensive Summaries of Uppsala Dissertations from the Faculty of Science and Technology 135

Numerical Methods for Aerodynamic Shape Optimization

OLIVIER AMOIGNON

ACTA
UNIVERSITATIS
UPSALIENSIS
UPPSALA
2005

ISSN 1651-6214
ISBN 91-554-6431-9
urn:nbn:se:uu:diva-6252

Dissertation presented at Uppsala University to be publicly examined in Pol 2/446, 2, Uppsala, Friday, January 20, 2006 at 10:00 for the degree of Doctor of Philosophy. The examination will be conducted in English.

Abstract
Amoignon, O. 2005. Numerical Methods for Aerodynamic Shape Optimization. Acta Universitatis Upsaliensis. *Digital Comprehensive Summaries of Uppsala Dissertations from the Faculty of Science and Technology* 135. viii+34 pp. Uppsala. ISBN 91-554-6431-9.

Gradient-based aerodynamic shape optimization, based on Computational Fluid Dynamics analysis of the flow, is a method that can automatically improve designs of aircraft components. The prospect is to reduce a cost function that reflects aerodynamic performances.

When the shape is described by a large number of parameters, the calculation of one gradient of the cost function is only feasible by recourse to techniques that are derived from the theory of optimal control. In order to obtain the best computational efficiency, the so called adjoint method is applied here on the complete mapping, from the parameters of design to the values of the cost function. The mapping considered here includes the Euler equations for compressible flow discretized on unstructured meshes by a median-dual finite-volume scheme, the primal-to-dual mesh transformation, the mesh deformation, and the parameterization. The results of the present research concern the detailed derivations of expressions, equations, and algorithms that are necessary to calculate the gradient of the cost function. The discrete adjoint of the Euler equations and the exact dual-to-primal transformation of the gradient have been implemented for 2D and 3D applications in the code Edge, a program of Computational Fluid Dynamics used by Swedish industries.

Moreover, techniques are proposed here in the aim to further reduce the computational cost of aerodynamic shape optimization. For instance, an interpolation scheme is derived based on Radial Basis Functions that can execute the deformation of unstructured meshes faster than methods based on an elliptic equation.

In order to improve the accuracy of the shape, obtained by numerical optimization, a moving mesh adaptation scheme is realized based on a variable diffusivity equation of Winslow type. This adaptation has been successfully applied on a simple case of shape optimization involving a supersonic flow. An interpolation technique has been derived based on a mollifier in order to improve the convergence of the coupled mesh-flow equations entering the adaptive scheme.

The method of adjoint derived here has also been applied successfully when coupling the Euler equations with the boundary-layer and parabolized stability equations, with the aim to delay the laminar-to-turbulent transition of the flow. The delay of transition is an efficient way to reduce the drag due to viscosity at high Reynolds numbers.

Keywords: Computational Fluid Dynamics, shape optimization, adjoint equations, edge-based finite-volume method, moving mesh adaptation, radial basis functions, inviscid compressible flow, transition control

Olivier Amoignon, Department of Information Technology, Box 337, Uppsala University, SE-75105 Uppsala, Sweden

ISSN 1651-6214
ISBN 91-554-6431-9
urn:nbn:se:uu:diva-6252 (http://urn.kb.se/resolve?urn=urn:nbn:se:uu:diva-6252)

To Anita, Mikael and Anna

List of Papers

This thesis is based on the following papers, which are referred to in the text by their Roman numerals.

I Amoignon, O., Berggren, M. (2005) Adjoint of a median-dual finite-volume scheme applied to 2D and 3D transonic aerodynamic shape optimization. Submitted to *Computers and Fluids*.

II Amoignon, O., Pralits, J.O., Hanifi, A., Berggren, M., Henningsson, D.S. (2005) Shape optimization for delay of laminar-turbulent transition. *AIAA Journal*, accepted for publication.

III Jackobson, S., Amoignon, O. (2005) Mesh Deformation using Radial Basis Functions for Gradient-based Aerodynamic Shape Optimization. Submitted to *Computers and Fluids*.

IV Amoignon, O. (2005) Moving Mesh Adaptation for Aerodynamic Shape Optimization. Submitted to *Journal of Computational Physics*.

Contents

1. Introduction

> "Without the knowledge of the theory of the air flow around airfoils it is well-nigh impossible to judge or interpret the results of experimental work intelligently or to make other than random improvements at the expense of much useless testing."
>
> Theodore Theodorsen, NACA TR-411, 1931

1.1 A short history of aerodynamic design

1.1.1 Before modern aviation

Flying has remained a mystery to mankind as long as the flight of birds found no explanation. Some of it could be eluded by one of Johan Bernoulli's (1667-1748) discoveries, that *the pressure in a fluid reduces as the speed increases*. Isaac Newton's laws (1643-1727) are equally advocated to explain lifting. The application of his laws yields, simply stated, that the deviation downward of the air flow around a wing is an effect of a force downward oriented and created by the shape of the wing. Therefore, this force will be equilibrated by a reaction force applied upward by the air on the wing.

But lack of physical explanations did not discourage inventors, among whom we find Leonardo Da Vinci (1452-1519) who drew sketches of flying machines mostly inspired from bird's morphology. But none of his machines ever flew, mostly because a man would not have the strength to power the mechanisms he designed, and also because his understanding of flying was not accurate.

The history of aviation began in the second half of the nineteenth century. In 1853, Great Britain, Sir George Cayley was first to fly a glider, followed by Otto Lilenthal (1848-1896) in Germany, whose studies and experiments on stability and aerodynamics influenced followers, see [30]. Among them, the Wright brothers, U.S.A., are the most famous. They succeeded with the first controlled flight of an engine powered airplane in 1903. The two brothers also conducted wind tunnel tests on many wing profiles, thus inaugurating experimental research on wing design.

1.1.2 Before modern computers

Following the Wright brothers, aeronautical engineers and designers for decades improved the performance of airplanes without the help of computers. Experimental work, through empirical laws as well as through wind tunnel tests, has driven this progress. Wind tunnel testings are still the ultimate step to go through before flight testings. However, the precursor of computer aided design is the human ability in mathematical modeling that allowed the prediction of rather complex flows around two dimensional geometries by help of the theory of potential flows and boundary layers.
Using potential flow theory and conformal mapping, Theodorsen [41], in 1931, calculated the velocity in an inviscid and incompressible fluid around airfoils. The solution of the inverse design problem, which aims at finding the shape if the pressure is given around the airfoil, is attributed to Lighthill [29], in 1945, who used the above named conformal mapping. It is therefore the real start for the numerical optimization of aerodynamic shapes, still without requiring a massive amount of calculations.

1.2 Design with Computational Fluid Dynamics

1.2.1 From inverse design to optimization

The method of Lighthill [29] was followed and developed by others [26]. However, the method of inverse designs supposes that the flow is known, at least partially. This is a serious limitation, because the prescribed pressures or velocities around the airfoil are not necessarily feasible solutions to the flow equations [26].

An alternative is to formulate the inverse design as a problem of optimization, where the target pressure p^t on the surface Γ of an airfoil is approximated as well as possible, for example by minimizing the cost function defined as the integral of the quantity $|p^t - p_\Gamma|^2$ on Γ. The formulation of the inverse problem as an optimization problem avoids the difficulty to find feasible target pressures.

Gradient-based optimization may efficiently minimize the cost function above, provided that the gradient of this function can also be calculated efficiently. Perturbation methods, such as divided differences, require as many flow solutions as there are parameters of design. In an *optimal control* approach, the gradient can be calculated by solving once an *adjoint* equation derived from the flow equations.

Design optimization using an optimal control approach has become popular in the last two decades in all fields of engineering. For a detailed presen-

tation of techniques of optimal shape design for systems governed by elliptic equations, the reader may refer to a book by Pironneau [36]. For an introduction focusing on aerodynamic shape optimization, the reader may refer to Giles & Pierce [22].

1.2.2 Adjoint equations in CFD

Concerning optimization based on Computational Fluid Dynamics (CFD) calculations, the use of the adjoint equations has become common in recent years [2, 5, 6, 8, 9, 13, 17, 27, 31, 33, 38, 39, 40].

There are however different views on the application of the theory of optimal control in CFD [25]. In the so-called continuous approach, the adjoint equations and the expression of the gradient are derived from the Partial Differential Equations (PDEs) that model the flow and from the exact cost function, see [5, 17, 27, 39, 40]. The resulting expressions are then discretized. In the so-called discrete approach, the adjoint equations and gradient expression are obtained from the discretized flow equations and cost function [2, 9, 13, 33].

In terms of efficiency of the optimization, the discrete approach may be preferred because it can provide the exact gradient of the cost function being optimized. Otherwise, lack of accuracy may cause a failure of the optimization algorithm in finding a descent direction. There are however some drawbacks to the discrete approach, for example concerning the meaning of the adjoint of artificial numerical fluxes like artificial viscosities [25]. Another positive aspect of the discrete approach is that the boundary conditions of the adjoint equations unfold naturally, whereas it may be difficult to formulate them when using the continuous approach [34]. Discussion about the two approaches can be found in a book by Gunzburger [25].

Results of aerodynamic shape optimization are obtained by the method of discrete adjoint in [2, 15, 21, 31, 32, 34], but little is reported about the discrete adjoint for the finite volume method used here. For results of aerodynamic shape optimization by a continuous approach, the reader may refer to [5, 11, 16, 28, 39, 40].

The major difference between discrete and continuous approach is thus that the numerical fluxes of the adjoint equations, in the discrete case, are imposed by the discretization of the flow equations. The unstructured type of discretization used in the CFD code Edge [12] has become popular because it allows an efficient calculation of the numerical fluxes on meshes that are inexpensive to produce, even for complicated geometries. Concerning an introduction to this discretization, we refer to Barth [3].

There are few studies [2, 13, 22] that have been concerned by developing the method of adjoint for unstructured finite-volume schemes similar to the

one used here. We do not find detailed expressions or derivations in those references, unless at an abstract level, of the complete adjoint equations and gradient expressions.

1.2.3 Automatic Differentiation

The tediousness involved in deriving the adjoint equations, by the discrete or the continuous approach, together with accuracy issues, may be the reasons that push forwards the developements of programs for the automated production of derivatives [19, 7, 20, 24, 37]. Briefly described, software of Automatic Differentiation (AD) produce a duplicated program, for example from the one that calculates the discretized flow equations (CFD), in which the algebraic expressions are symbolically differentiated.

There are, for the time being, some limitations to AD. For instance, the memory requirements in the so-called reverse mode, which corresponds to an adjoint solution, restricts the applicability for large problems [31].

2. Summary of papers

2.1 Paper I

This paper presents in details the derivation of the adjoint equations and the gradient of the cost function with respect to the design parameters, when the flow state is the solution of the discretized Euler equations in Edge [12]. These expressions have been implemented and tested in order to enable optimization of shapes in 2D and 3D, when the flow analysis is executed by solving the compressible Euler equations on unstructured grids.

2.1.1 Discrete sensitivities

To become more familiar with the general idea behind the adjoint approach applied to the discretized optimization problem presented in this paper, consider first a simpler problem in the spirit of Giles & Pierce [22]. Let a cost function J be linear with respect to the vector of state variables $\mathbf{w}$,

$$J(\mathbf{w}) = \mathbf{g}^T \mathbf{w}\,, \tag{2.1}$$

with $\mathbf{g} \in \mathbb{R}^n$ given and $\mathbf{w} \in \mathbb{R}^n$ subject to the state equation

$$\mathrm{A}\mathbf{w} = \mathrm{N}\mathbf{a}\,, \tag{2.2}$$

where $\mathbf{a} \in \mathbb{R}^m$ is the vector of design variables, $\mathrm{A} \in \mathbb{R}^{n\times n}$, and $\mathrm{N} \in \mathbb{R}^{n\times m}$.

Assume that A is nonsingular. The reduced gradient of J, that is, the gradient of the mapping $\mathbf{a} \mapsto J(\mathbf{w}(\mathbf{a}))$, denoted ∇J_a, may be obtained by solving the *sensitivity equations* of the state: given a variation of the control variable $\delta\mathbf{a}$, corresponding variation of the state $\delta\mathbf{w}$ is defined as the solution to the sensitivity equations

$$\mathrm{A}\,\delta\mathbf{w} = \mathrm{N}\,\delta\mathbf{a}\,, \tag{2.3}$$

which enables us to express the variation of the function J

$$\delta J = \mathbf{g}^T \delta\mathbf{w} \equiv \mathbf{g}^T \mathrm{A}^{-1}\mathrm{N}\,\delta\mathbf{a}\,. \tag{2.4}$$

Therefore, solving the sensitivity equations, once for each component of the vector $\mathbf{a}$, yields the gradient ∇J_a, component by component.

However, rewriting (2.4) as

$$\delta J = \left(\mathrm{N}^T \mathrm{A}^{-T} \mathbf{g}\right)^T \delta \mathbf{a}\,, \tag{2.5}$$

reveals that replacing $\mathrm{A}^{-T}\mathbf{g}$ in (2.5) by the adjoint state $\mathbf{w}^*$, defined as the solution to

$$\mathrm{A}^T \mathbf{w}^* = \mathbf{g}\,, \tag{2.6}$$

gives an expression for ∇J_a,

$$\nabla J_a = \mathrm{N}^T \mathbf{w}^*\,. \tag{2.7}$$

The cost for computing the gradient by expression (2.7) is one costate solution (2.6), instead of m solutions of the sensitivity equations (2.3) when expression (2.4) is used.

The generalization to nonlinear state equations and nonlinear functions J is straightforward:

- $\mathbf{g}$ is the vector of partial derivatives of the function J with respect to the vector of the state variables $\mathbf{w}$,
- A is the Jacobian matrix of the system of state equations with respect to the state variables,
- N is the Jacobian matrix of the system of state equations with respect to the control variable, which, in the formulation of Edge, is the set of data of the median-dual mesh ($\mathbf{n}_h$).

2.1.2 Edge-based finite-volume discretization

The derivation of the adjoint of the Euler equations discretized in the CFD code Edge follows the ideas exposed in the previous section (§ 2.1.1). By a perturbation technique, the cost function, as well as the system of Euler equations, are linearized with respect to the flow variables and the mesh data. However, the Jacobians are not available as matrices for efficiency reasons. Therefore, the transposition of the Jacobians, which is the crucial step in order to express the adjoint equations, is carried out through a discrete analogue of integration by parts.

A crucial tool for the concise derivation of the edge-based scheme that assembles of the numerical fluxes in the adjoint equation is Lemma 1, which provides a relation between different ways of summing algebraic expressions defined on unstructured meshes:

Lemma 1 *Let $G \equiv (V, A)$ be an oriented graph, in which V is the list of vertices (i) and A is the list of edges (i, j). Let $\mathcal{N}_i$, for each vertex $i \neq j$ in V, be the list of vertices j in V such that there is an edge in A connecting i and j.*

Given a list of edge-based data $\{\mathbf{e}_{ij}, \mathbf{e}_{ji}\}_{\vec{ij}\in A}$*, it holds that*

$$\sum_{i\in V}\sum_{j\in\mathcal{N}_i}\mathbf{e}_{ij} = \sum_{\vec{ij}\in A}\left[\mathbf{e}_{ij}+\mathbf{e}_{ji}\right] .$$

The final expression of the gradient with respect to the data of the median-dual mesh (the set of surface normal vectors associated with the dual control volumes), is obtained from the definition of an adjoint equation like (2.6), and the product of the Jacobian of the discretized Euler equations with respect to the data of the median-dual mesh, the equivalent operation to (2.7).

The use of the median-dual grid requires a pre-processing of the element mesh data in order to obtain the surface normals of the control volumes, also called the dual data in the paper. In order to calculate the gradient with respect to the primal grid, that is, with respect to the nodal coordinates, the chain rule can be applied. As in the pre-processing, the element topology is needed when applying the chain rule. The algorithm that is derived here calculates the partial derivatives of the cost function with respect to the mesh coordinates from the partial derivatives with respect to the dual mesh data.

2.1.3 Optimization in 2D and 3D

As an example of drag (C_D) minimization in 2D, the RAE 2822 airfoil is re-designed at transonic speed, given here by the Mach number $M_\infty = 0.734$, and for an angle of attack $\alpha = 2.19^o$. The design parameters (224 parameters in the numerical experiments shown here) specify the normal displacements on the airfoil through the solution of a Quadratic Programming problem. This parameterization [1] includes linear constraints on the geometry, like a constant cross-section area, in addition to the fixed position of the trailing edge. Lift and pitching moment coefficients are held constant by adding penalty terms to the cost function. The results of this optimization are shown in Figure 2.1. The pressure drag is reduced by 75 drag counts, while the lift and pitching moment are kept within 1%, in comparison with the values for the RAE 2822 airfoil. In a 2D inviscid compressible flow, the drag is due to the presence of shocks. The shock is indeed efficiently smoothened at final design (Figure 2.1).

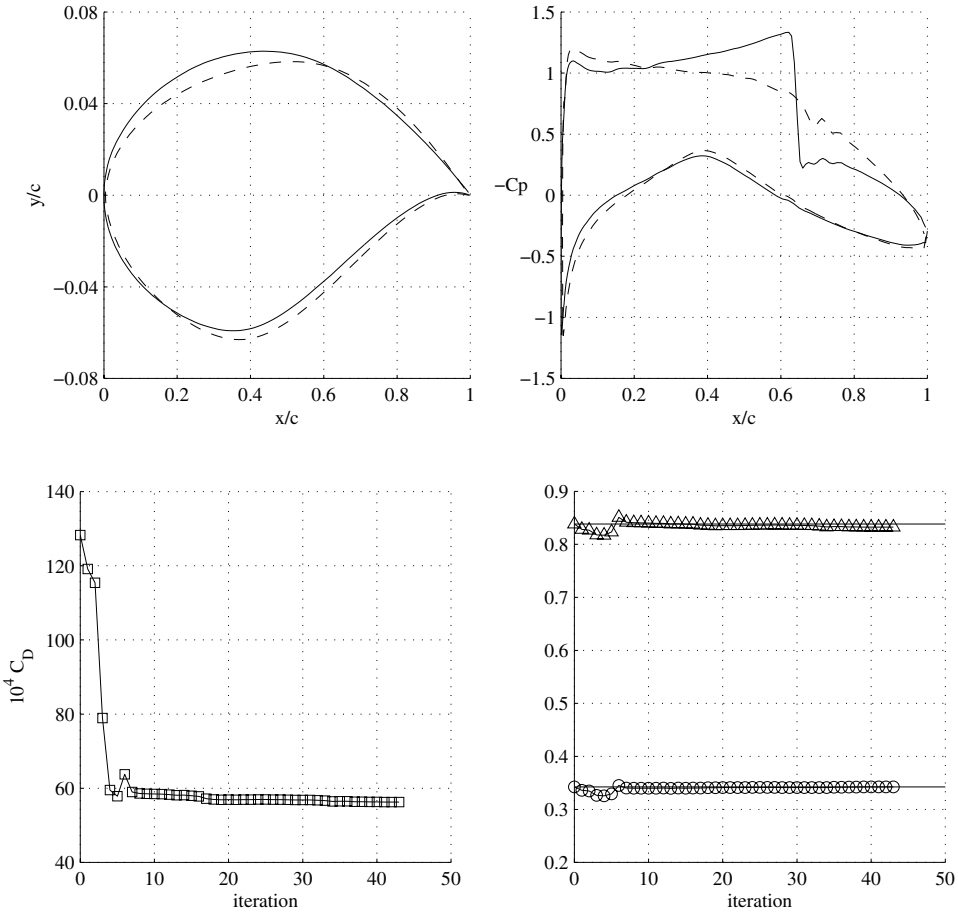

Figure 2.1: Upper left: RAE 2822 airfoil (solid) and final design (dashed). Upper right: pressure coefficient on the RAE 2822 (solid) and on the final design (dashed). Lower left: drag counts at each design ($10^4 \cdot C_D$). Lower right: lift coefficient (triangles) and pitching moment (circles) at each design.

An example of drag minimization in 3D is given by the re-design of the ONERA M6 wing at Mach number $M_\infty = 0.8395$ and angle of attack $\alpha = 3.06^o$. In the example shown here, the parameterization consists of a decomposition of the spanwise distribution of the camber, the twist, and the thicknesses, in terms of splines. In this case (TCT-6s) the drag is reduced by about 30 drag

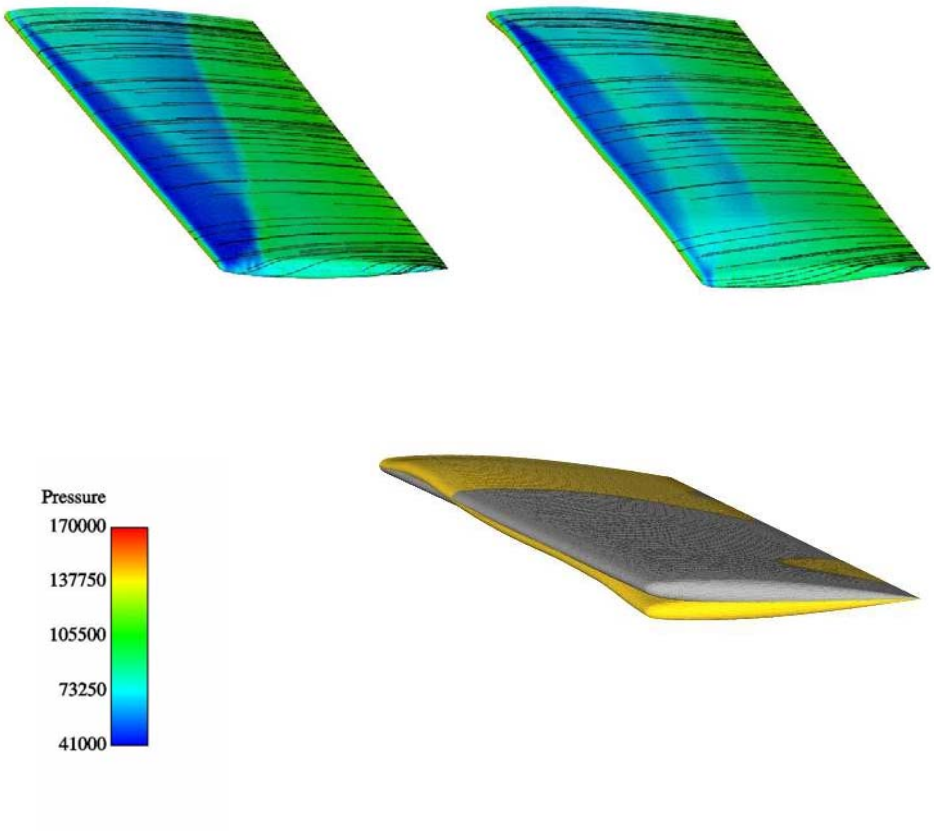

Figure 2.2: Case TCT-6s. Upper left: pressure contours on the ONERA M6 wing. Upper right: pressure contours on the final design. Bottom: superposed geometry of the ONERA M6 wing (grey, dark grey in BW) and of the final design (yellow, light grey in BW).

counts, the lift varies of about 1% and the pitch varies with less than 0.02%. The two shocks are visibly smoothened (Figure 2.2) and the vortex at the tip is shifted downstream, which is known also to reduce the drag. The shape of the final design is characteristic of all the tests that were carried out here on the M6 wing. The local angle of attack is increased near the root of the wing and decreased towards the tip of the wing. The changes in the local angle of attack is a combination of the twist deformation, around the trailing edge, and of the camber. There are, however, differences in the profiles of the wings

depending on the number of splines and depending on the type of the parameterization. These differences do not affect much the performances of the final designs, meaning that all the design succeed to reduce the drag and maintain the lift and pitch with about the same amplitudes.

2.2 Paper II

The aim of this paper is to extend the use of adjoint-based optimization developed for active laminar flow control [18] to natural laminar flow design. The same optimal control approach as in Paper I is used, but instead of a cost function that depends explicitly on the solution of the Euler equations, we introduce a cost function that depends only implicitly on the Euler flow. The cost function is the kinetic energy of one disturbance in the laminar boundary layer on the upper part of an airfoil. In order to calculate the values of this kinetic energy, the Euler equations are coupled to the mean flow equations in the boundary layer (BLE) and the parabolized stability equations (PSE). Section 2.2.1 presents the principle of the calculations of the disturbance kinetic energy and of the calculation of the shape gradient of this energy. In order to couple the three state equations, constraints on the possible shapes were imposed through the parameterization as explained in Section 2.2.2. This method of parameterization is the same than the one used in Paper I and was proposed in [1]. The results obtained in this paper show that the reduction of the energy of one disturbance efficiently reduces the energy of 'all' unstable disturbances, which is assumed to represent a delay of the transition of the flow from laminar to turbulent in the boundary layer. Section 2.2.3 presents a short discussion of those results.

2.2.1 Disturbance energy and shape gradient

The three state equations are sequentially coupled, and we neglect the viscous-inviscid interactions. This assumption greatly facilitates the calculation of the gradient by the adjoints of the Euler equations, boundary layer equation and parabolized stability equation, see Figure 2.3. Furthermore, by analyzing the growth of disturbances based on the pressure calculated by the Reynolds-averaged Navier-Stokes equations, instead of the Euler equations, we could verify that neglecting the viscous-inviscid interaction has small effects on our results, see Section 2.2.3.

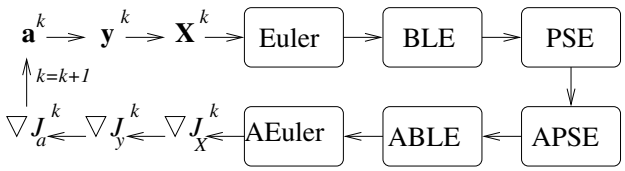

Figure 2.3: Flow chart for the case of minimizing the disturbance kinetic energy.

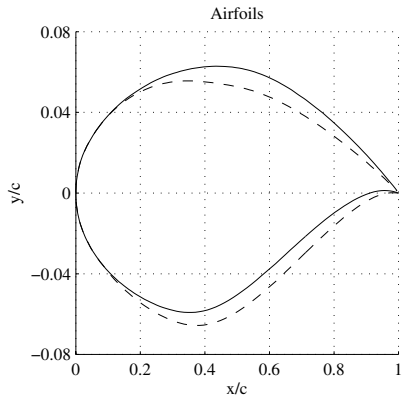

Figure 2.4: T11 - Comparison between initial (solid) and final design (dash).

2.2.2 Parameterization

Freezing a small part of the geometry of the airfoil in the neighborhood of the stagnation point, that is, around the leading edge, was a necessary condition for the coupling of the Euler equations with the equations that model the mean viscous flow and the propagation of instabilities in the boundary layer. If we had limited the study to the reduction of the disturbance kinetic energy, it would have been sufficient to parameterize the upper part of the airfoil, where the boundary layer analysis takes place, and keep the rest of the wing fixed. However, our aim was to simultaneously reduce the kinetic energy of the disturbance as well as the pressure drag, while imposing constraints on the lift and the pitching moment coefficients. Having in mind that imposing constraints in optimization induces a reduction of the set of feasible designs, it was considered wise to work with as large a set of designs as possible. This is the reason why we used the technique of parameterization proposed in [1]. By this technique we can obtain smooth updates of the shape, together with a constraint on the 'volume' of the airfoil (cross-sectional area), and impose the displacements normal to the wing to vanish in a small region around the stagnation point as shown in Figure 2.4.

2.2.3 Results

The e^N-method attempts to predict the location of the transition from the calculation of a large number of disturbances. By this approach, the location at which the Envelope-of-Envelope (EoE) of N-factor curves, obtained from all the calculated kinetic energies, reaches some empirical value, is the location of the transition. An example of EoE curves obtained on the final design, after minimization of the kinetic energy of one disturbance, is shown in Figure 2.5.

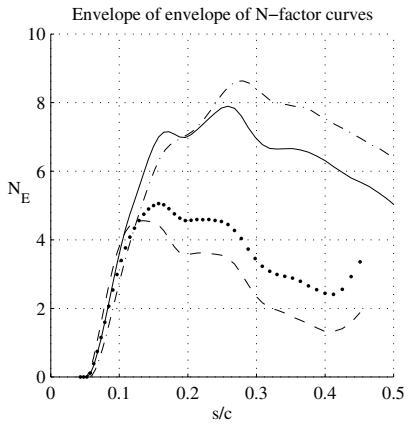

Figure 2.5: T11 - EoE of N-factor curves: at initial design(solid) and final design (dash). EoE of N-factor curves involving the RANS equations are shown for the initial (dash-dot) and final (dot) design.

If the transition would occure at the value $N_E = 7$, for example, the transition would occure at the non-dimensional curvilinear coordinate $s/c = 0.15$, on the initial design, and it would not occure at all on the final design. Note that the transition can occure outside of the domain of calculation of the equations in the boundary layer (here $0 \leq s/c \leq 0.5$). Similar results were obtained when using the RANS equations, instead of the Euler equations, for the analysis of the EoE curves, see Figure 2.5. This last result confirms that it was appropriate to neglect the viscous-inviscid interaction for the numerical experiments shown here.

2.3 Paper III

Paper III proposes an efficient method to deform unstructured 2D and 3D meshes, and gives a detailed presentation of all aspects of the implementation for gradient-based aerodynamic shape optimization. Section 2.3.1 briefly describes the method and its use in the context of aerodynamic shape optimization. Performances of the new method are analyzed, as summarized in Section 2.3.2. The results of shape optimization obtained in the paper are commented in Section 2.3.3.

2.3.1 Geometrical interpolation

The problem of deformation of the mesh is recasted in the framework of interpolation of scattered data. Control nodes are chosen among the nodes that discretize the shape to optimize and the mapping from the positions of those control nodes ($\boldsymbol{x}_{k_i}$) to the displacements of all other node in each direction (v_x, v_y, v_z) is defined from an interpolant. The construction of the interpolant is based on radial basis functions (ϕ):

$$v_x = s_x(\boldsymbol{x}) = \sum_{i=1}^{N} \gamma_i^x \phi(\|\boldsymbol{x} - \boldsymbol{x}_{k_i}\|) + \beta_1^x + \beta_2^x x + \beta_3^x y + \beta_4^x z,$$

$$v_y = s_y(\boldsymbol{x}) = \sum_{i=1}^{N} \gamma_i^y \phi(\|\boldsymbol{x} - \boldsymbol{x}_{k_i}\|) + \beta_1^y + \beta_2^y x + \beta_3^y y + \beta_4^y z,$$

$$v_x = s_z(\boldsymbol{x}) = \sum_{i=1}^{N} \gamma_i^z \phi(\|\boldsymbol{x} - \boldsymbol{x}_{k_i}\|) + \beta_1^z + \beta_2^z x + \beta_3^z y + \beta_4^z z,$$

As a result, the displacement of a node on the wing, other than a control node, is obtained by interpolation. The displacement of all other nodes in the interior of the domain of computation is an extrapolation.

An example of mesh deformation in 2D, without constraints at the domain boundaries, is shown in Figure 2.6. In CFD applications, constraints are needed at far-field and symmetry boundaries, for example. The modification of the interpolation method, in order to account for those additional constraints, is detailed in the paper.

For an efficient implementation in aerodynamic shape optimization, the *forward* mapping executing the deformation of the mesh must be supplemented by a *backward* or adjoint mapping that provides the gradient of the cost function with respect to the boundary nodes on the parameterized shape. In the present method of mesh deformation, the backward mapping is given by the chain rule for which details are found in the article.

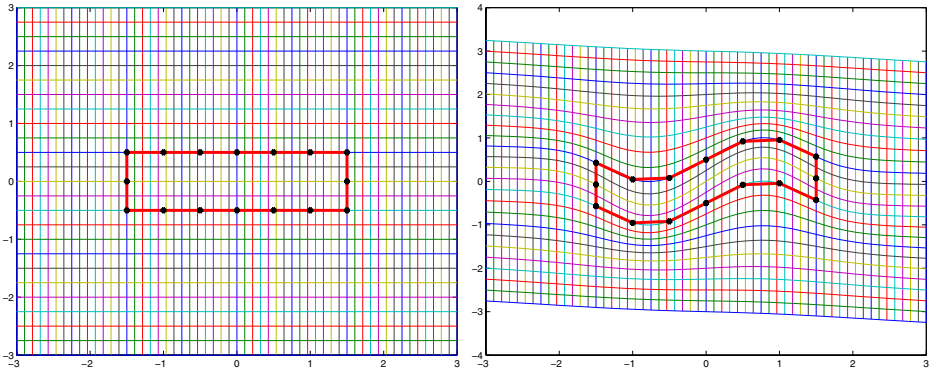

Figure 2.6: Left: the undeformed domain and the control nodes. Right: deformation resulting from a sinusoidal deflection of the control nodes.

2.3.2 Performances

The computational time required by the interpolation method to deform a mesh is compared to the time required by solving an elliptic equation suitable for mesh deformation (a method described in Paper I). As explained ealier, the displacements of the nodes on the parameterized shape are interpolated from the displacements of the control nodes. The trade-off between computational cost and numerical accuracy is thus an important factor when comparing the interpolation method to another method of mesh deformation.

The results, in the case of the deformation of a 3D Euler mesh for the ONERA M6 wing, indicate a factor 2 to 10 in favor of the interpolation method (RBF), for a maximum relative error of order 10^{-3} on the position of the nodes on the parameterized wing. In fact, the relative errors do not vary much when changing the number of control nodes (here from 2166 down to 730), so that the proposed method is one order of magnitude faster than solving an elliptic mesh smoother on the 3D Euler mesh (solved with the tolerance 10^{-7}).

In the case of the deformation of the 3D mesh for the ONERA M6 wing for RANS calculations, following the same observation on the small influence of the number of control nodes on the relatives error, we obtain a speed-up of a factor 30 by the new method in comparison with solving an elliptic equation (solved with the tolerance 10^{-7}).

The noticeable difference of results between the computational times obtained for the meshes of Euler type and RANS type is due to the highly stretched elements in the RANS mesh, which causes difficulties in solving elliptic equations.

The mesh qualities give another important information about the performance of a mesh deformation method. The tests are carried out with various parameters that characterize the interpolation method, such as the type of ra-

dial basis functions, a so-called shape parameter, and the number of control nodes. The qualities of the deformed meshes are, except for a few cases, similar to the qualities of the undeformed mesh. In a few cases, where the shape factor of the radial basis functions is small, the maximum aspect ratio, among all deformed elements in the mesh, can be large, or, elements can be inverted.

2.3.3 Gradient-based shape optimization

The same optimization of the ONERA M6 wing as in Paper I is carried out, replacing the mesh deformation based on elliptic smoothing used in Paper I by the interpolation scheme. The results of optimization obtained through the two methods are very close to each other. The explanation for the small differences is given by the analysis of the performance discussed above. That is, the method of interpolation approximates the shape given by the parameterization, in contrast to the mesh deformation based on the elliptic equation, which uses the information given by the parameterization at every node on the wing. The difference in the mesh qualities of the meshes deformed by the two methods may also contribute to the small differences.

2.4 Paper IV

Paper IV proposes a mesh adaptation scheme for gradient-based aerodynamic shape optimization. The goal is to achieve a better accuracy of the shape obtained by optimization, compared to the shape that solves the exact problem of optimization. The method is inspired by moving mesh algorithms used for the adaptation of the mesh in unsteady problems involving flows with discontinuities, like shocks. The originality of the proposed method is to replace the solution of the flow equations by a coupled flow and mesh equation.

2.4.1 Moving mesh adaptation

The mesh node coordinates ($\mathbf{X} = [\mathbf{X}'', \mathbf{X}']$) are defined as the solution to a non-linear elliptic equation with variable diffusivity, which can be described by the system of equations

$$\begin{bmatrix} \mathrm{A}(\mathbf{X}) & \mathrm{C}(\mathbf{X}) \\ 0 & \mathrm{B}(\mathbf{X}) \end{bmatrix} \begin{bmatrix} \mathbf{X}'' \\ \mathbf{X}' \end{bmatrix} = \begin{bmatrix} \mathbf{0} \\ \mathbf{g}' \end{bmatrix} \qquad \begin{matrix} (\mathbf{X}'' \text{: interior nodes coor.}) \\ (\mathbf{X}' \text{: boundary nodes coor.}) \end{matrix}$$

The entries of the block matrices $(\mathrm{A}, \mathrm{B}, \mathrm{C})$ are functions of the coordinates $(\mathbf{X})$ through a diffusivity function m. In order to control the mesh densities, the diffusivity is a function of the flow solution, computed on the mesh described by $\mathbf{X}$, through an indicator of the error. As a result, we solve the coupled mesh and flow equations simultaneously in order to obtain the adapted mesh and flow solutions for a given design ($\mathbf{g}'$).

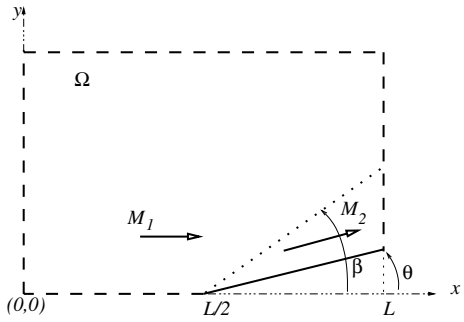

Figure 2.7: Inviscid supersonic flow past a wedge.

The method is applied on the CFD calculation of a supersonic flow over a wedge with half-angle θ, see Figure 2.7. The adaptation improves the accuracy of the calculated drag, in comparison with uniform mesh refinement, see Figure 2.8.

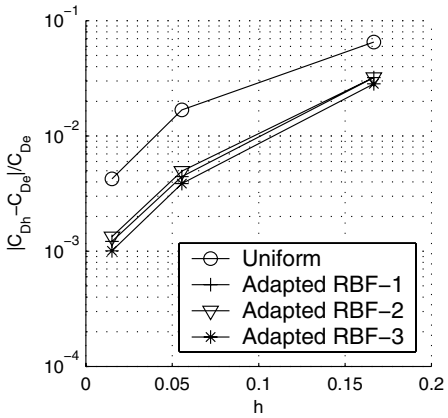

Figure 2.8: Grid convergence towards the exact drag on a wedge at $M_1 = 2.5$, $\theta = 15^o$, with uniform grids and with adapted grids (RBF-1,2,3).

2.4.2 A 2D inverse problem

The flow over a wedge is used to build a benchmark for testing the accuracy of the shape optimization. In some intervals of angles and Mach numbers, there is a one-to-one relation between the angle of the wedge (θ) and the drag on the wedge. We derive, from this observation, an inverse design problem with a known exact solution (θ_{exact}). By solving the problem of optimization on a uniform grid we can compare the calculated angle of the optimal shape to the exact solution of the inverse problem (Figure 2.9). The uniform grid convergence of the calculated angle is comparable to the uniform grid convergence of the calculated drag, see Figure 2.8. The proposed approach consists of

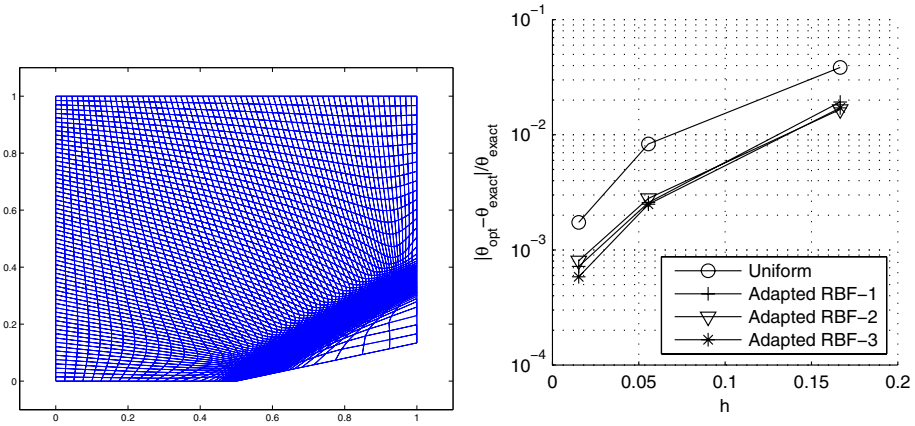

Figure 2.9: Left: final adapted mesh at $M_1 = 2.5$ and calculated optimal angle $\theta_{\text{opt}} = 15.0088^o$. Right: comparison between the exact optimal wedge angle ($\theta_{\text{exact}} = 15^o$) and the numerical optimum angle (θ_{opt}) with our without adaptation.

replacing the flow calculation on uniform grids by the calculation of the coupled mesh and flow equations in the optimization algorithm. The result of the optimization, the calculated optimal angle θ_{opt}, is improved (see Figure 2.9) in the same manner as the drag calculation in Figure 2.8.

2.4.3 Solution algorithm

When solving the coupled mesh-flow equations, at a given iteration of the algorithm the flow is solved approximately, and the coefficients of the mesh equation are calculated from the pressure in the flow through a sensor and the diffusivity function. The solution of these coupled non-linear equations by an approximate Newton method with underrelaxation converges slowly or not al all ('Alg2' in Figure 2.10).

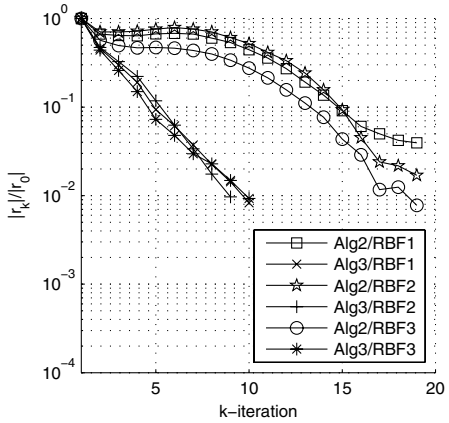

Figure 2.10: Convergence of the coupled Euler-Moving Mesh equations using an approximate Newton method (Alg2) and a modified approximate Newton method (Alg3) based on interpolation of the mesh equation coefficients RBF (1, 2 or 3).

A possible explanation is the decoupling of the mesh updates from the flow variables. This decoupling would yield large displacements of the nodes, whereas the flow solution, in particular the position of the shock, is rather insensitive to the mesh. A method based on the interpolation of the coefficients of the mesh equation is derived using radial basis functions. In all tests, the resulting algorithm ('Alg3' in Figure 2.10) converges faster than the approximate Newton without interpolation.

3. Perspectives

3.1 From Euler to RANS

The most obvious continuation of the present work would be the application of the adjoint method to the equations for compressible viscous flows at large Reynolds numbers, modeled by the Reynolds-averaged Navier-Stokes equations (RANS). The use of the RANS equations in aerodynamic shape optimization, with or without turbulence models, is reported in several publications [31, 28, 14, 35, 34]. Note that the numerical schemes used there are presented at an abstract level or derived from other methods than the explicit formulation of the adjoint equations [31, 35], for instance by automatic differentiation.

In order to calculate the gradients of the cost functions used in Paper I–IV, when the flow is solution of the RANS equations discretized in Edge, we would need the following:

- The adjoint of the numerical fluxes that arise from the discretization of the molecular viscosity terms in the equations.
- The sensitivities of the same numerical fluxes with respect to the grid data.

For the calculation of the shape gradient of cost functions term that include the shear-stress, the corresponding forcing term of the adjoint equations must be derived.

Other practical details concerning the derivation of the adjoint of the viscous fluxes are discussed in a report by Giles [21]. For example, he proposes a method of projection that facilitates the transposition of the Jacobians when the no-slip boundary condition applies.

3.2 Error estimates in mesh adaptation

The main result of Paper IV is a procedure of *mesh adaptation*, by relocation of the positions of the nodes, that can be integrated in the process of gradient-based shape optimization. The motivation is to improve the accuracy of the shape obtained by numerical optimization, by improving the accuracy of the numerical approximation of the cost function.

The main ingredient of the adaptation procedure is a variable diffusion mapping, which gives a mean to control the mesh densities by a diffusion, a posi-

tive scalar field in the flow domain.

The example of flow used in Paper IV in order to illustrate this approach, facilitated the construction of a variable diffusivity, because the only feature of the flow is the shock. By choosing a sensor, the shock can be localized and a diffusivity built by convoluting the sensor with a compactly supported radial basis function.

For more complicated inviscid and viscous flows, the places in the mesh where the discretization needs to be refined are not necessarily limited to regions of 'strong gradients' of the flow solution.

Therefore, in order to extend to more complicated flows the adaptation method presented in Paper IV, one could study the possibility of using *a posteriori* error estimates such as used in [42, 23, 4] for deferred correction and $h-$adaptation.

3.3 Interpolation of scattered data

Two techniques of interpolation based on Radial Basis Functions are derived and applied in Paper III and IV in different contexts.

The interpolation of Paper III has been used for the deformation of unstructured meshes. It was emphasized that the technique is derived from a more general problem that also applies to the coupling of the flow equations with the equations of structural analysis, as it occurs in aeroelasticity. The parameterization of shapes is another application than can enter in the description of the above-named general problem of interpolation (see Paper III).

In Paper IV the method of interpolation is used to efficiently solve the coupled mesh and flow equations. The interpolant is the discrete convolution of a sensor and a radial basis function. An implementation for large-scale applications (large CFD meshes) would require a fast algorithm for calculations involving the convolution. Methods such like the fast multipole method and moment-based methods may be possible candidates.

3.4 Shape parameterization with constraints

The technique introduced in [1] and used in Paper I and Paper II for parameterization of airfoil shapes is analogous to the *obstacle problem* of structural mechanics for a thin elastic string. By this analogy, the forces are parameters of design, and the obstacle, which is a constraint in the variational formulation of the problem [10], is replaced by one or several linear constraints on the normal displacements of the string. The difference with the obstacle problem is that the linear constraints are defined as equalities, which makes the resulting quadratic program (QP) particularly easy to solve. This formulation of

the displacements allowed to fix the linearized volume of the airfoil optimized in [1] and in Paper I, and to fix part of the optimized airfoil around the leading edge in Paper II. This technique enabled smooth updates of the shapes during optimization without reduction of the number of degrees of freedom, unless those conceded to the geometrical constraints.

Another advantage of this approach is to transform (geometrical) constraints of the problem of optimization into parameters of design. Furthermore, the solution of the adjoint of this QP problem, which is solved in order to obtain the gradient with respect to the design parameters, also gives the partial derivatives with respect to the geometrical constraints. To summarize, the shape parameterization, derived in 2D, has the following characteristics:

- The parameterization mapping takes the form of a linear system of equations (QP) on the boundary.
- The gradient-based updates of the shape are smooth without loss of information from the gradient.
- Linear equality constraints on the shape are transformed into parameters of design.
- The partial derivatives of the cost function with respect to the geometrical constraints are obtained from the solution of the adjoint (QP) problem.

A next step would be to extend this technique to 3D optimization. In this case, the displacements normal to the surface of the wing would be analogous to the normal displacements of a flexible membrane.

4. Summary in Swedish: Numeriska metoder för aerodynamisk formoptimering

Under flygning skapar luftströmmen runt flygplanet krafter som genererar lyft, men också motstånd samt deformationer av flygkroppen. Kunskap om dessa fenomen är grundläggande för att ingenjörer ska kunna utveckla säkra flygplan med låga driftskostnader.

Aerodynamiska datorsimuleringar för flygplanstillämpningar kan vara tillräckligt noggranna under vissa strömningsförhållanden som till exempel vid marchfart. Med hjälp av datorsimuleringar kan aerodynamiska egenskaper av preliminära flygplansmodeller testas. För varje ny modell kan varianter testas i syfte att förbättra dess egenskaper på ett tidigt stadium i utvecklingsprocessen. Möjligheten att automatiskt förbättra formen av flygplansdelar är en lockande men utmanande uppgift.

Ett effektivt sätt att förbättra former är att använda numerisk optimering. Formen av en vinge, till exempel, beskrivs av ett antal parametrar som specificerar dess längd, tjocklek och krökning. Eftersom även små ändringar i formen kan ha en stor betydelse för flygplanets prestanda är det viktigt att kunna använda noggranna beskrivningar av de flygplansdelar som skall förbättras. Det innebär att hundratals parametrar kan behöva justeras. Gradientbaserade algoritmer för optimering är effektiva för att minimera en funktion även när den beror på många parametrar. Eftersom optimeringen kräver upprepade simuleringar av strömningen är det viktigt att algoritmen för att beräkna gradienten är effektiv.

Det finns olika sätt att ta fram gradienten av en kostfunktion inom aerodynamisk formoptimering. I en av metoderna görs en liten ändring av en designparameter och simuleringen av strömningen ger den störda kostnaden. Att jämföra den störda kostnaden med kostnaden för den ursprungliga designen ger en komponent av gradienten. Störningsmetoder är “dyra” eftersom gradienten har lika många komponenter som antalet parametrar och behöver räknas ut många gånger under optimeringen. Ett känt alternativ är att lösa så kallade adjunktsekvationer. Med hjälp av dessa kan gradienten beräknas effektivt oavsett antalet parametrar.

Artikel I presenterar de mest grundläggande resultaten i avhandlingen. Som påpekas ovan är störningsanalys ett viktigt steg i gradientbaserad

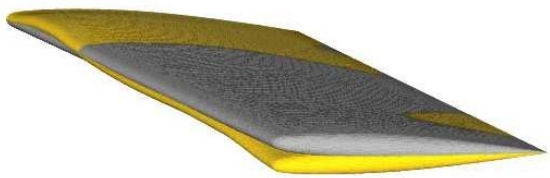

Figure 4.1: I grått (mörkgrå i SV) visas formen av ONERA M6-vingen. Den gula formen (ljusgrå i SV) får man genom att minimera motståndet med konstant lyft och vridmoment. Parametrarna som används här styr formen på ett sätt som tillåter krökningen, tjockleken och den lokala anfallsvinkeln att variera spännvis (från roten till spetsen av vingen).

aerodynamisk formoptimering. I den analysen härleds uttryck för gradienter av funktioner som motstånd, lyftkraft eller moment. Gradienten beräknas effektivt genom att lösa adjunktsekvationer till de linearisera strömningsekvationerna. Strömningsmodellen ges av Eulerekvationerna för en kompressibel gas som löses numeriskt i Edge, ett program för strömningsmekaniska beräkningar på ostruktuerade nät. Adjunktsekvationen och gradientutrycket härleds från den diskreta avbildning som inkluderar strömningsekvationen, nätförsjutningsalgoritmen och parametriseringen av formen. Här presenteras en metod för att härleda adjunktsekvationen för den kantbaserade finita-volymsdiskretisering som används i Edge såväl som i många andra beräkningsprogram inom flygindustrin. Kantbaserade diskretiseringsmetoder lämpar sig särkilt bra för att effektivt beräkna strömningsfälten runt komplicerade geometrier. Ett exempel av en optimerad vinge som presenteras i artikeln visas i figur 4.1. På den optimerade vingen är luftmotståndet 20% lägre än för den ursprungliga vingen.

I artikel II tillämpas liknande metoder som i artikel I för att optimera en vingprofil med avseendet på störningsenergin i gränsskiktet närmast vingsprofilens yta, med avsikt att fördröja omslag från laminär till turbulent strömning. Den inviskösa strömningen fås genom att lösa Eulerekvationerna för kompressibel strömning. Den laminära grundströmningen fås genom att lösa gränsskiktsekvationerna för kompressibel strömning på oändligt svepta vingar. Tillväxten av konvektivt instabila störningar analyseras med hjälp av lin-

jära stabilitetsekvationer i parabolisk form (PSE). Analysen av den formoptimerade vingprofilen visar en minskning av den totala tillväxten av ett stort antal störningar vilket antas representera en fördröjning av laminär-turbulent omslag. Då en fördröjning av omslaget innebär en minskning av det viskösa motståndet, är formoptimeringsproblemet som presenteras här en ny metod för att genomföra minimering av det viskösa motståndet. Metoden har inte för avsikt att dämpa den turbulenta strömningen utan förlitar sig på modellering av störningars spridning och tillväxt i den laminära delen av gränsskiktet. Liknande resultat fås också då tryckmotståndet och störningsenergin samtidigt reduceras medan lyft och vridmoment behålls nära initiala värden.

För både gradientbaserad aerodynamisk optimering och aeroelasticitet (kopplade struktur- och strömningsberäkningar) behövs snabba metoder för nätdeformering. I artikel III presenteras en interpolationsmetod baserad på radiella basfunktioner (RBF) för att propagera förkjutningarna av noderna på randen av beräkningsnätet till det inre. Metoden kan minska beräkningskostnaden för nätdeformationen jämfört med deformationsmetoder baserade på lösningar av den diskreta Laplaceekvationen (*Laplace Smoothing*). Algoritmen använder ej strukturen hos nätet. Därför kan strukturerade, ostrukturerade samt hybridnät behandlas likvärdigt. Tillämpningar på aerodynamisk formoptimering är också undersökta. För gradientbaserade optimeringsalgoritmer skall kostfunktionen deriveras med avseende på designparametrarna. För aerodynamisk formoptimering beräknas gradienten effektivast och noggrannast med den adjungerade ekvationen till de diskretiserade strömningsekvationerna som presenteras i artikel I. Beräkningen av gradienten använder Jacobianmatrisen för nätdeformeringen vilket beskrivs i detalj i rapporten.

Slutligen presenteras resultatet av optimering av ONERA M6-vingen i transonisk fart med interpolationsalgoritmen och jämförs med Laplacetekniken för nätdeformation. Kvaliten på beräkningsnätet och interpolationsfelet jämförs för olika parametrar till interpolationsschemat: typen av basfunktion, skalparametern till basfunktionen samt olika mängder av kontrollpunkter.

Adaptionsmetoden som presenteras i artikel IV anpassar nätet till det beräknade strömningsfältet utan att förändra uppdelningen av nätet i olika element. Detta är viktigt för att adaption ska kunna användas för gradientbaserad formoptimering. I denna typ av metod, som kallas r-adaption, förändras enbart nodernas koordinater, i motsats till så kallad h-adaption. Koordinaterna i nätet är lösningen till en icke-linear elliptisk ekvation inspererad från Winslows variabla diffusivitetsekvation. Nätekvationen och strömingsekvationen är kopplade för att nodernas koordinater ska anpassas till strömningen och lösningen till strömningsekvationen ska uppdateras efter ändringarna i beräkningsnätet. Koppligen sker via en diffusivitetfunktion som byggs på faltningen av en sensor med en radiell basfunktion. Användningen av sensorn

är ett enkelt sätt att lokalisera interpolationsfel i närvaron av diskontinuerliga lösningar. Den radiella basfunktionen som används har kompakt stöd och är kontinuerlig. Faltningen används för att diffusiviteten ska variera kontinuerligt i rummet. Numeriska experiment med den adaptiva metoden tillämpad på överljudsströmning över en kil—ett modellproblem för strömning med diskontinuiteter—visar att det beräknade motståndet är bättre approximerat på det adaptiva nätet. Som konsekvens av denna förbättring blir lösningen till ett inversproblem byggd på motståndet också mer noggrant beräknad.

Acknowledgments

Many thanks to my advisor Martin Berggren for his support during this thesis. His tutoring was excellent in every details, from the initiation to the 'adjoint' and 'gradient' derivation for some finite element discretization to much broader discussions on every aspects of the numerics involved here.

I am thanksfull to all the staff of the Division of Scientific Computing (TDB), in Uppsala, for the friendly atmosphere and the very good quality of the lectures and seminars.

An important part of this work has been performed at the Swedish Defense Research Institute (FOI), which is nowadays the authority for the development and support of the program Edge. I thank Torsten Berglind and Peter Eliasson for giving me the opportunity to work at FOI, in the framework of my graduate studies as well as on other projects, which has greatly facilitated the developments I did on the code Edge. FOI has also been the place where my collaborations took place. In particular, I want to thank Jan Pralits, Stefan Jakobsson, and Adam Jirasek.

Thanks to Anita for her help and understanding, and to our kids, Mikael, eight and Anna, a big three-and-a-half, who on Sunday mornings took care of us better than we did take care of them the rest of the week.

Funding from the Parallel and Scientific Computing Institute (PSCI) is greatly acknowledged. This research has received support from the AEROSHAPE project funded by the European Commission, DG Research, under the GROWTH initiative (Project Ref: GRD1-1999-10752). Partial support for this research has been obtained through the Department of Energy, USA, for my visit at CSRI.

References

[1] O. Amoignon. Adjoint-based aerodynamic shape optimization. Technical Report IT Licentiate theses 2003-012, Department of Information Technology, Division of Scientific Computing, Uppsala University, Box 337, SE-751 05 Uppsala, Sweden, October 2003.

[2] W.K. Anderson and D.L. Bonhaus. Airfoil design on unstructured grids for turbulent flows. *AIAA Journal*, 37(2):185–191, 1999.

[3] T.J. Barth. Aspects of unstructured grids and finite-volume solvers for the Euler and Navier–Stokes equations. In *Special Course on Unstructured Methods for Advection Dominated Flows*, pages 6–1–6–61. AGARD Report 787, May 1991.

[4] T.J. Barth. *A posteriori* error estimate and mesh adaptivity for finite volume and finite element methods. *Springer series Lecture Notes in Computational Science and Engineering*, 41:1–21, 2004.

[5] O. Baysal and K. Ghayour. Continuous adjoint sensitivities for optimization with general cost functionals on unstructured meshes. *AIAA Journal*, 39(1):48–55, 2001.

[6] F. Beux and A. Dervieux. Exact-gradient shape optimization of a 2D Euler flow. Technical Report RR-1540, INRIA Sophia Antipolis, 2004 Route des Lucioles, 06360 Valbonne, France, 1991.

[7] C.H. Bischof, A. Carle, P. Hovland, P. Khademi, and A.XS Mauer. Adifor 2.0 user's guide (revision d). Technical Report 192, Mathematics and Computer Science Division, Argonne National Laboratory, 1998.

[8] G. Bugeda and E. Oñate. Optimum aerodynamic shape design for fluid flow problems including mesh adaptivity. *Int. J. Numer. Meth. Fluids*, 30:161–178, 1999.

[9] G.W. Burgreen and O. Baysal. Three-dimensional aerodynamic shape optimization using discrete sensitivity analysis. *AIAA Journal*, 34(9):1761–1170, 1996.

[10] P. G. Ciarlet. *The Finite Element Method for Elliptic Problems*. North-Holland, Amsterdam, 1978.

[11] G. Cowles and L. Martinelli. A control-theory based method for shape design in incompressible viscous flow using rans. *AIAA Paper*, 2000.

[12] P. Eliasson. Edge, a Navier–Stokes solver, for unstructured grids. Technical Report FOI-R–0298–SE, Swedish Defence Research Agency, Stockholm, November 2001.

[13] J. Elliot and J. Peraire. Aerodynamic design using unstructured meshes. *AIAA Paper*, (96-1941), 1996.

[14] J. Elliot and J. Peraire. Aerodynamic optimization on unstructured meshes with viscous effects. *AIAA Paper*, (97-1849), 1997. 13th AIAA CFD Conference, Snowmass, Colorado, June, 1997.

[15] J. Elliot and J. Peraire. Constrained, multipoint shape optimization for complex 3D configurations. *The Aeronautical Journal*, pages 365–376, August/September 1998. Paper no. 2375.

[16] O. Enoksson. Shape optimization in compressible inviscid flow. Licenciate Thesis LiU-TEK-LIC-2000:31, 2000. Department of Mathematics, Institute of Technology, Linköpings University.

[17] O. Enoksson and P. Weinerfelt. Numerical methods for aerodynamic optimization. Proceedings to the 8th International Symposium on Computational Fluid Dynamics, 5-10 Sept., Bremen, 1999.

[18] J.O. Pralits et al. Adjoint-based optimization of steady suction for disturbance control in incompressible flows. *J. Fluid Mech.*, 467:129–161, 2002.

[19] C. Faure and Y. Pegay. Odyssée user's guide version 1.7. Technical Report RT-0224, INRIA, 1998. URL http://www-sop.inria.fr/tropics/tapenade.html).

[20] R. Giering and T. Kaminski. Recipes for adjoint code construction. *ACM Tans. Math. Software*, 24(4):437–474, 1998.

[21] M.B. Giles. Algorithm developments for discrete adjoint methods. Technical Report 01/15, Oxford University Computing Laboratory, Numerical Analysis Group, Wolfson Building, Parks Road, Oxford, England OX1 3QD, 2001.

[22] M.B. Giles and N.A. Pierce. An introduction to the adjoint approach to design. *Flow, Turbulence and Combustion*, 65:393–415, 2000.

[23] M.B. Giles and N.A. Pierce. Adjoint error correction for integral outputs. In *Error Estimation and Adaptive Discretization Methods in Computational Fluid Dynamics*, volume 25. In Lecture Notes in Computational Science and Engineering, Springer, 2002.

[24] A. Griewank, D. Juedes, H. Mitev, J. Utke, O. Vogel, and A. Walther. ADOL-C: A package for the automatic differentiation of algorithms written in C/C++. *ACM TOMS*, 22(2):131–167, 1996. Algor. 755.

[25] M.D. Gunzburger. *Perspectives in Flow Control and Optimization*. Society for Industrial and Applied Mathematics, Philadelphia, PA, USA, 2002.

[26] A. Jameson. Aerodynamic design via control theory. *Journal of Scientific Computing*, 3:233–260, 1988.

[27] A. Jameson and S. Kim. Reduction of the adjoint gradient formula for aerodynamic shape optimization problems. *AIAA Journal*, 41(11), 2003.

[28] A. Jameson, N.A. Pierce, and L. Martinelly. Optimum aerodynamic design using the Navier-Stokes equations. *AIAA Paper*, (97-0101), 1997.

[29] M.J. Lighthill. A new method of two-dimensional aerodynamic design. Technical report, ARC, 1945.

[30] O. Lilienthal. *Birdflight as the Basis of Aviation*. Longmans, Green & Co., 1911. Translation from "Der Vogelflug als Grundlage der Fliegekunst". Berlin: R. Gaertners Verlag, 1889.

[31] B. Mohammadi. A new optimal shape procedure for inviscid and viscous turbulent flows. *Int. J. Numer. Meth. Fluids*, 25:183–203, 1997.

[32] B. Mohammadi and O. Pironneau. Mesh adaption and automatic differentiation in a CAD-free framework for optimal shape design. *Int. J. Numer. Meth. Fluids*, 30:127–136, 1999.

[33] S.K. Nadarajah. *The discrete adjoint approach to aerodynamic shape optimization*. PhD thesis, Aeronautics and Astronautics Department, University of Stanford, 2003.

[34] S.K. Nadarajah and A. Jameson. Studies of the continuous and discrete adjoint approaches to viscous automatic aerodynamic shape optimization. *AIAA Paper*, (2001-2530), 2001.

[35] M. Nemec and D.W. Zingg. Towards efficient aerodynamic shape optimization based on the Navier–Stokes equations. *AIAA Paper*, (2001-2532), 2001.

[36] O. Pironneau. *Optimal Shape Design for Elliptic Systems*. Springer Verlag, 1984.

[37] O. Pironneau and N. Di Césaré. Flow control problem using automatic differentiation in C++. LAN-UPMC report 99013, 1999. Laboratoire d'Analyse Numérique, Université Pierre et Marie Curie, Paris VI, France. URL: http://acm.emath.fr/ dicesare/cpp.php3.

[38] J. J. Reuther, A. Jameson, J. J. Alonso, M. J. Rimlinger, and D. Saunders. Constrained multipoint aerodynamic shape optimization using an adjoint formulation and parallel computers, part 1. *J. Aircraft*, 36(1):51–60, 1999.

[39] B.I. Soemarwoto. *Multi-Point Aerodynamic Design by Optimization*. PhD thesis, Delft University of Technology, Faculty of Aerospace Engineering, P.O. Box 5058, 2600 GB Delft, Netherlands, 1996.

[40] C. Sung and J.H. Kwon. Accurate aerodynamic sensitivity analysis using adjoint equations. *AIAA Journal*, 38(2):243–250, 2000.

[41] T. Theodorsen. Theory of wing sections of arbitrary shapes. Technical Report NACA/TR-411, Langley Memorial Aeronautical Laboratory, National Advisory Committee for Aeronautics, Langley Field, Virginia, USA, October 1931.

[42] D.A. Venditti and D.L. Darmofal. Adjoint error estimation and grid adaptation for functional outputs: Application to quasi-one-dimensional flow. *Journal of Computational Physics*, 164(1):204–227, October 2000.

Acta Universitatis Upsaliensis

Digital Comprehensive Summaries of Uppsala Dissertations from the Faculty of Science and Technology 135

Editor: The Dean of the Faculty of Science and Technology

A doctoral dissertation from the Faculty of Science and Technology, Uppsala University, is usually a summary of a number of papers. A few copies of the complete dissertation are kept at major Swedish research libraries, while the summary alone is distributed internationally through the series Digital Comprehensive Summaries of Uppsala Dissertations from the Faculty of Science and Technology. (Prior to January, 2005, the series was published under the title "Comprehensive Summaries of Uppsala Dissertations from the Faculty of Science and Technology".)

Distribution: publications.uu.se
urn:nbn:se:uu:diva-6252

ACTA
UNIVERSITATIS
UPSALIENSIS
UPPSALA
2005